

# DEVELOPMENT OF A THERMAL CONDUCTANCE INSTRUMENT FOR NIOBIUM AT CRYOGENIC TEMPERATURES

Cem Saribal\*, C. Martens, M. Wenskat, W. Hillert  
Universität Hamburg, Hamburg, Germany

## Abstract

Particle accelerators form an important tool in a variety of research fields. In an effort to reduce operation costs while maintaining high energies, their accelerating structures are steadily improved towards higher accelerating fields and lower RF losses. Stable operation of such a cavity generally requires Joule-heating, generated in its walls, to be conducted to an outer helium bath. Therefore, it is of interest to experimentally evaluate how present and future cavity treatments affect thermal characteristics. We present an instrument for measuring the thermal performance of SRF cavity materials at cryogenic temperatures. Pairs of niobium disks are placed inside of a liquid helium bath and a temperature gradient is generated across them to obtain total thermal resistance for temperatures below 2 K. To get an idea of the instruments sensitivity and how standard cavity treatments influence thermal resistance, samples are tested post fabrication, polishing and 800 °C baking. The first tests show the commissioning of our newly set up system and if it is feasible to observe relevant changes and evaluate new and promising cavity treatments such as SIS structures.

## INTRODUCTION

The thermal performance of accelerating structures not only influences achievable accelerating fields, but also affects operation costs, which for the most part are given by the cryoplant. As the rf field interacts with normal conducting electrons on the inner surface of the cavity walls, heat is generated due to surface resistance. This undesirable power dissipation in form of so-called Joule-heating increases surface temperature and reduces quality factor. At sufficiently large fields heat cannot be conducted to the outer helium bath effectively anymore, leading to a sudden decrease of cavity performance.

In order to push breakdown towards its theoretical maximum field it is mandatory to avoid thermal feedback, deteriorating the rf performance before its inherent limitations. The thermal resistance of a cavity, which determines the cavities response to surface heating, is comprised of two components. First the resistance of the bulk material determines how freely heat flows from the inner surface, where it is created, through the metal and to the outer surface. For a homogeneous bulk this resistance linearly depends on thickness. The second component is given by the resistance at the interface between cavity wall and liquid helium bath. In typical cavities at cryogenic temperatures these resistances often are comparable to each other in magnitude and their sum makes up the total thermal resistance.

\* cem.saribal@studium.uni-hamburg.de

Here, we present the current development status of our Niobium Thermal Conductance Instrument (NTCI), a thermal conduction instrument for niobium at cryogenic temperatures. Its design is based on a similar device, which was first introduced and utilized by J. Amrit, M.X. François and C.Z. Antoine over two decades ago [1, 2]. In comparison to standard thermal conduction instruments, which most of the time are limited to thermal characteristics of the bulk, this design additionally allows taking interface resistance into account, which makes results better applicable to the real world thermal behaviour of cavities. Therefore, NTCI also allows to study the impact of 10 – 100 nm thin layers, effectively representing only a fraction of the whole volume, on total thermal resistance.

## EXPERIMENTAL SETUP

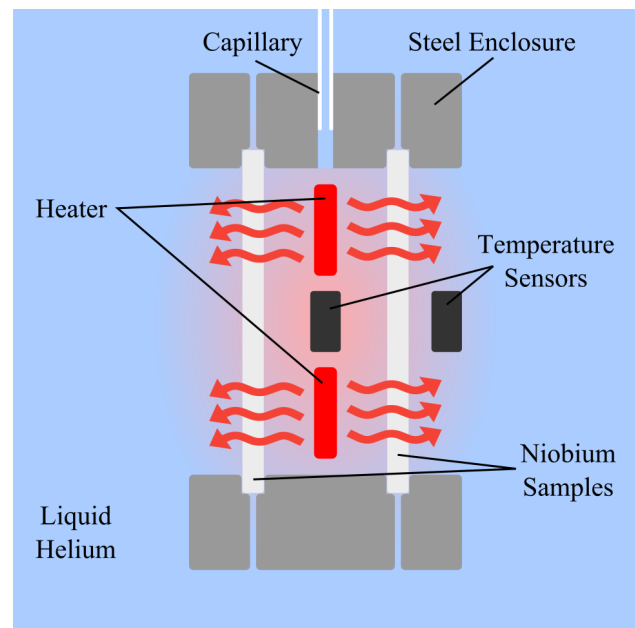


Figure 1: Cross-sectional view of NTCI.

The fundamental working principle of NTCI can be understood by looking at its cross-section shown in Fig. 1. A pair of identically treated disc-shaped niobium samples with a diameter of 45 mm is mounted to a ring-shaped steel enclosure with a wall thickness of 20 mm, creating a 16 mm deep cylindrical cavity with a diameter of 40 mm in-between the samples. Inside of this cavity a heating element, consisting of a 1 m long Manganin wire with 0.1 mm diameter is symmetrically wound in a 3D-printed fixture, resulting in an electrical resistance of about 50 Ω. In its center this fixture houses a Cernox CU-HT temperature sensor (see

Content from this work may be used under the terms of the CC BY 4.0 licence (© 2023). Any distribution of this work must maintain attribution to the author(s), title of the work, publisher, and DOI

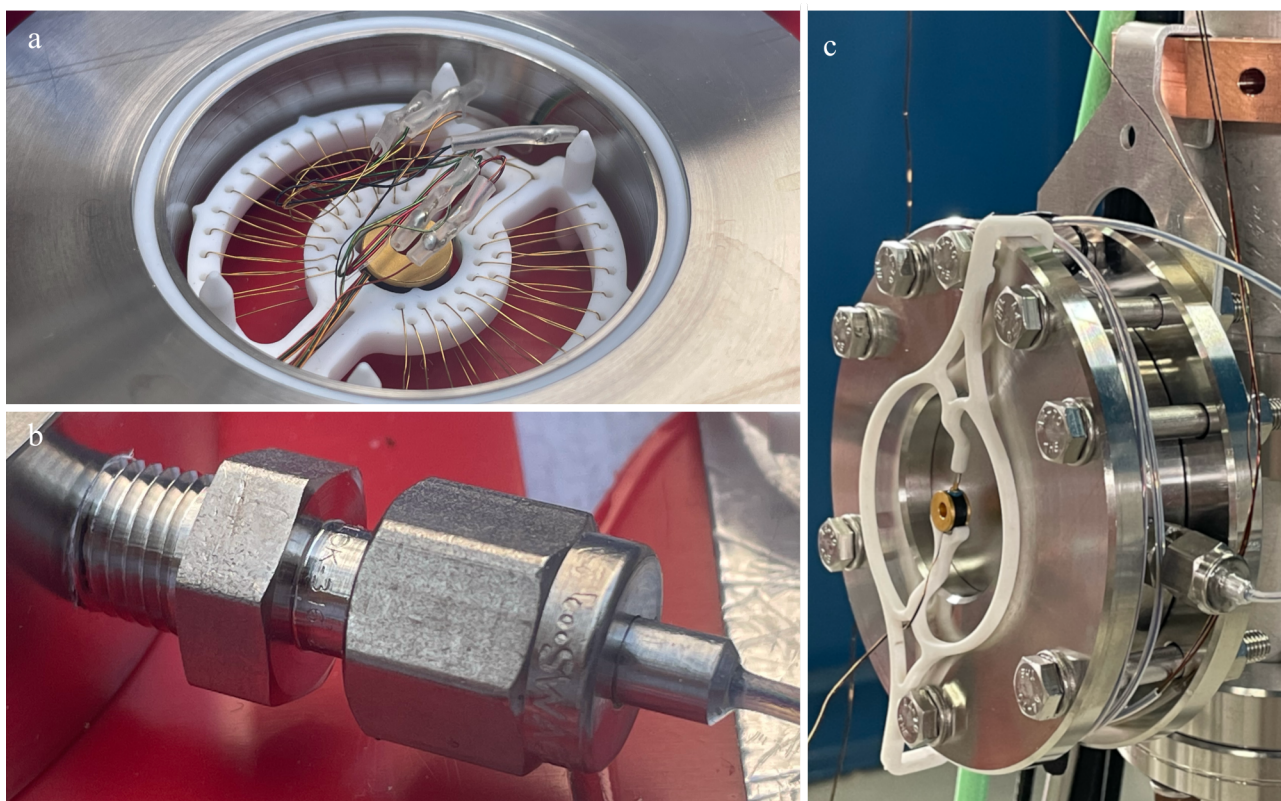


Figure 2: Images of NTCI. (a) Inner cavity containing heating element and temperature sensor. (b) Screwed connection between inside and outside. (c) Fully assembled instrument mounted to insert.

Fig. 2 a). Through a small hole in the round surface of the steel enclosure the inner cavity is connected to the outside. A screwed connection followed by a 1 m long PTFE capillary with an inner diameter of 1 mm serves as a filling line for superfluid helium as well as the copper wires needed for inner electronics (see Fig. 2 b). Outside and about 3 mm from the outer surface of one of the samples a second Cernox CU-HT temperature sensor is installed with another 3D-printed fixture. The fully assembled instrument, which can be seen in Fig. 2 c, is mounted to a cryostat insert at the accelerator module test facility at DESY. To control the heating element and read out temperature sensors a Model 336 Cryogenic Temperature Controller from Lakeshore is utilized. Accurate heating power is obtained by measuring heater current and voltage with two 6 1/2 digit multimeters.

In an ideal setup heat flow only occurs through the niobium samples and average thermal resistance can be obtained by reducing Fourier's Law to one dimension and assuming a constant conductance throughout the whole sample as shown in Equation 1. Here  $q = P_{heater}/(2A_{cavity})$  represents heat flux, which further breaks down into heating power,  $P_{heater}$ , and cross-sectional area of the inner cavity,  $A_{cavity}$ . Thermal resistance is given by  $R$  and  $\Delta T$  describes the temperature difference between inner and outer helium bath. In real world, however, heat can also take other paths from the inner helium bath to the outer one. These additional paths are intrinsically given by the construction and comprised of helium filling

line capillary, stainless steel enclosure and copper wires of inner electronics. The former path represents the largest heat loss source due to the relatively large thermal conductivity of superfluid helium. Losses through it are estimated to less than 5%, based on peak heat flux calculations for turbulent heat transport in superfluid helium channels [3]. Further losses through stainless steel enclosure have been estimated to less than 0.5% by inserting reasonable values for heating power and temperature difference into Eq. (1). Similarly losses through the copper wiring have been estimated to less than 0.1%.

$$q = \frac{\Delta T}{R} \quad (1)$$

## MEASUREMENT & EVALUATION PROTOCOL

To evaluate the thermal characteristics of a given sample pair two measurement procedures are utilized. In order to find out how thermal resistance qualitatively changes as a function of sample temperature a constant heating power is applied, while varying cryostat temperature,  $T_o$ . Example results for this scenario are shown in Fig. 3 for a constant heating power of 300 mW. Here, one can see temperature of inner liquid helium bath,  $T_i$ , cryostat temperature,  $T_o$ , and thermal resistance,  $R$ , as functions of time. To obtain more precise values for  $R$  at typical cavity operation temperatures

a second measurement procedure is carried out at constant  $T_o$  and by varying  $P_{heater}$  as seen in Fig. 4. Here, one can see a step-wise increase of heating power over time up to about 500 mW at a cryostat temperature of roughly 2 K. It is visible that  $R$  increases with increasing  $P_{heater}$ , suggesting the existence of additional paths of heat flow in the form of leaks with heat flux dependent activity, which need to be considered.

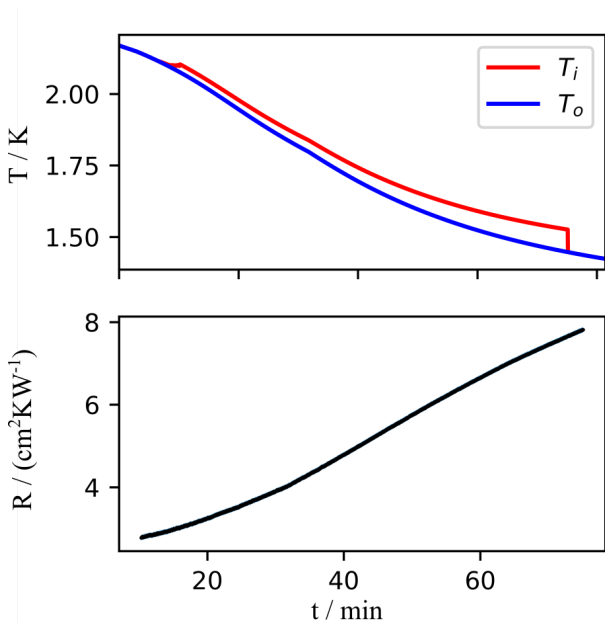


Figure 3: Exemplary data for measurements at variable cryostat temperature and constant heating power. Temperature of inner liquid helium bath,  $T_i$ , cryostat temperature,  $T_o$ , and thermal resistance,  $R$ , are shown as functions of time.

In a leak free setup, which only allows heat flow through samples, steel enclosure and filling line capillary, thermal resistance is expected to be independent of heating power, if  $(T_i - T_o) \ll T_o$ , since here the relative temperature-dependent change in  $R$  can be neglected. The increase of thermal resistance with regard to  $P_{heater}$ , observed in the last row of Fig. 4, can be reasoned with heat loss through microscopic leaks, when considering the Gorter-Mellink heat transfer regime in superfluid liquid helium [3]. In this regime the thermal conductivity of the helium decreases with increasing heat flux by enhancing the mutual friction between normal and superfluid components. To nonetheless obtain thermal resistance of the sample pair it, therefore, is necessary to expand  $R$ . Here, it is helpful to picture different paths of heat flow as resistances, which are in parallel to each other (see Fig. 5).

Similar to its electrical counterpart the inverse of total thermal resistance can be obtained by adding up the inverse resistances,  $R_i$  of all available heat flow paths. To get rid of inverses one can switch to the conductance picture, since conductance,  $K$ , is equal to the inverse of  $R$ . Consequently Eq. (1) is expanded into Eq. (2). Here the first term of the right-hand side,  $K_{samples}$ , represents the average conduc-

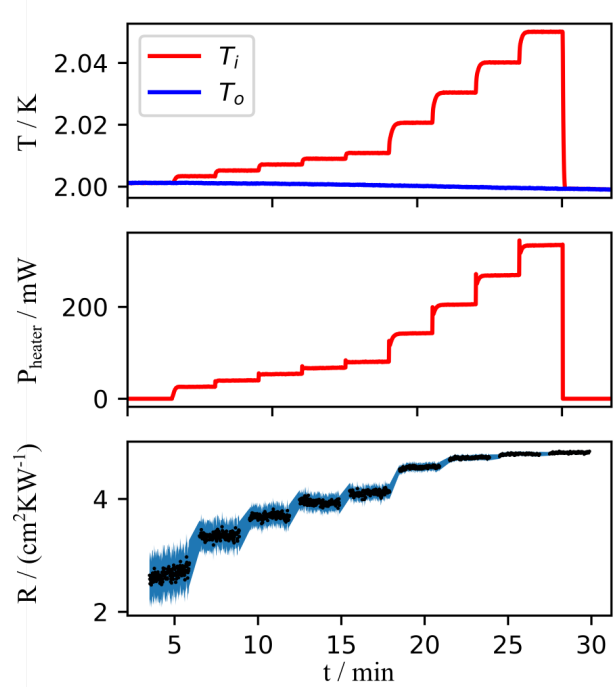


Figure 4: Exemplary data for measurements at constant cryostat temperature and variable heating power. Temperature of inner liquid helium bath,  $T_i$ , cryostat temperature,  $T_o$ , heating power,  $P_{heater}$ , and thermal resistance,  $R$ , are shown as functions of time.

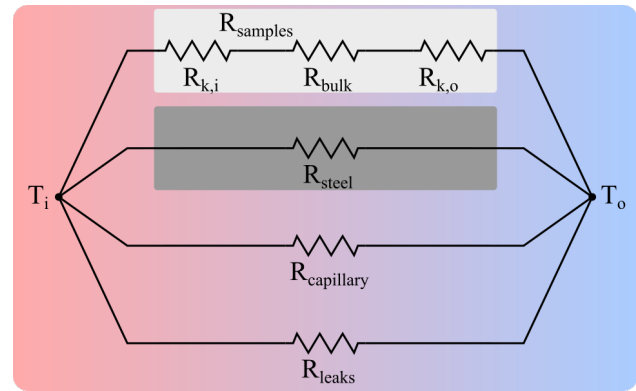


Figure 5: Resistance picture of heat flow paths.

tance of the sample pair and the quantity of interest. The second term describes an empirical fit for the total conductance of the leaks, which is readily used to approximate the thermal conductivity of liquid helium in thin capillaries. In this term  $a$  and  $n$  represent fitting parameters. The conductance of filling line capillary and steel enclosure are neglected, due to their comparably low influence.

$$\frac{q}{\Delta T} = K \approx K_{samples} + aq^{-n} \quad (2)$$

When fitting the right-hand side of Equation 2 to data measured at constant  $T_o$  and variable  $P_{heater}$ , (see Fig. 4), one obtains conductance fit curves as seen in Fig. 6. Here, results for measurements at 1.52 K, 1.80 K and 2.00 K cryostat



temperature with up to 500 mW of heating power are visible, which for all  $T_o$  at large heat fluxes converge towards  $K_{samples}(T_o)$ . In Table 1 resulting values for  $a$  and  $n$  are shown for cryostat temperatures of 2.00 K and 1.80 K and for different cool downs. Values for measurements taken at 1.5 K cryostat temperature are omitted, because of instabilities in  $T_o$ . The value obtained for  $n$  generally lies in-between 1.2 and 1.8, which is noticeably less than values of up to 4.0, found in literature [3]. The same applies to  $a$ , which results in a value three orders of magnitude smaller. This deviation most likely is a result of leaks in NTCI not resembling cylindrical tunnels, but rather slits with arbitrary changes in cross-sectional area along their paths. These slits are suspected to predominantly lie in the screwed connection (see Fig. 2 c), since it offers multiple surfaces of contact through which superfluid helium can leak. To investigate this assumption slight changes have been made to it in-between cool downs. In-between cool down four and five, for example, one of the contact areas has been wetted with liquid glue. As a result  $n$  stabilized around 1.7 at both cryostat temperatures. In-between cool down five and six additionally the screwed connection has been tightened by another half turn, leading to a noticeable decrease of both  $a$  and  $n$ .

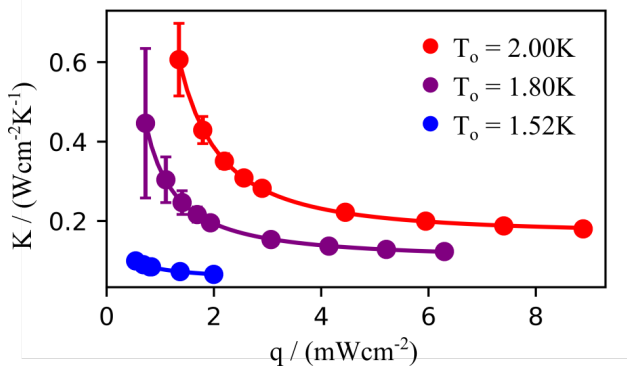


Figure 6: Exemplary conductance fits (solid lines) for data (dots) measured at different heating powers and cryostat temperatures.

Table 1: Fit Parameter Values for Different Cool Downs and Cryostat Temperatures

Cool Down #	2.00 K		1.80 K	
	a	n	a	n
4	0.74	1.77	0.23	1.31
5	2.14	1.72	1.21	1.69
6	0.14	1.25	0.09	1.26

## BASELINE STUDY

In order to evaluate the sensitivity of NTCI and find out, if it can be used to measure how conventional cavity treatments affect thermal resistance, a baseline is established. It consists of measurements for samples as fabricated, post

100  $\mu\text{m}$  buffered chemical polishing (BCP) and post 800  $^\circ\text{C}$  outgassing for 3 h (baking). Sample conductances,  $K_{samples}$ , obtained from fits and their 3-sigma deviations can be seen in Table 2. The given deviations not only take instrumental and statistical errors into consideration, but also account for systematic ones, which mostly result from the existence of leaks and are approximated to 3% of  $K_{samples}$ . The first line shows a measured thermal conductance of  $0.326 \text{ Wcm}^{-2}\text{K}^{-1}$  post fabrication, which consists of water-jet cutting all samples from one sheet of fine-grain niobium with 330 RRR and a thickness of about 2.65 mm. In the second line results post BCP are given. Here,  $K_{samples}$  decreases by about 14% down to  $0.280 \text{ Wcm}^{-2}\text{K}^{-1}$ . In the third line conductance post baking is shown, which decreases by another 28% down to  $0.199 \text{ Wcm}^{-2}\text{K}^{-1}$ . The sample pair used here is the same as in the post fabrication measurement of the first line. The number right next to treatment type refers to the treatment run. The last line represents measurements for a sample pair, which has been chemically polished separately to the samples of the two lines above and additionally baked in a different oven. Its conductance of  $0.167 \text{ Wcm}^2/\text{K}$  is relatively close to the value measured for the similarly but independently treated pair of samples in line three.

Assuming that bulk thermal resistance makes up half of total resistance, a bulk thermal conductivity of about  $0.172 \text{ Wcm}^{-1}\text{K}^{-1}$  is approximated for as fabricated samples. This agrees with the value of about  $0.150 \text{ Wcm}^{-1}\text{K}^{-1}$ , which has been found for niobium with a slightly lower RRR value in the past [4]. Therefore, conductance values delivered by NTCI seem to be comparable to what has been obtained with other instruments. The decrease in  $K_{samples}$  post BCP can be explained by impurities in form of hydrogen atoms diffusing into the metal. These impurities form additional scattering sites at the sample surface for heat carrying phonons and electrons, lowering their mean free path and, therefore, lowering total thermal conductance. The cause for further decrease in conductance post baking is not identified yet. Due to reproducing this effect for sample pairs baked similarly in different ovens, it is assumed that this reduction is not an artifact of possibly low instrument precision. The lower  $K_{samples}$ , measured after the first treatment run, is suspected to be a result of higher temperatures during BCP. In the first BCP run the acid bath temperature exceeded 25  $^\circ\text{C}$ , while it was kept below 14  $^\circ\text{C}$  during the second one, allowing less interstitial hydrogen to be introduced into the metal.

Table 2: Baseline Measurements at 2 K Cryostat Temperature

Sample Pair	Treatment	$K_{samples}$ ( $\text{Wcm}^{-2}\text{K}^{-1}$ )	$3\sigma$
A	fabrication	0.326	0.030
B	BCP 2	0.280	0.026
A	BCP 2 + baking 2	0.199	0.018
C	BCP 1 + baking 1	0.167	0.016

## CONCLUSION & OUTLOOK

An instrument for measuring the thermal performance of niobium in cryogenic environments, called NTCI, is successfully commissioned. Baseline studies show, that it is sensitive towards changes in total thermal resistance, introduced by readily used cavity treatments such as coarse buffered chemical polishing and 800 °C outgassing for 3 h. While it is reasonable to say that coarse BCP reduces thermal performance due to the diffusion of hydrogen, the cause of conductance reduction post outgassing remains unclear. Further investigations with regard to possible vacuum contamination during baking can be of insight.

To enhance accuracy of NTCI leaks can be investigated further by applying gradual changes in-between cool downs. Here, for example, the screwed connection can be gradually tightened with larger torques and other liquid adhesives, such as Stycast, can be used to improve the sealing at critical contact surfaces. Additionally one can test, if tightening the steel enclosure with different torques affects leak behaviour. If no such changes are introduced in-between cool downs, the instrument must be handled as cautious as possible in order to avoid altering existing leaks or adding new ones and to preserve precision. Moving on from the baseline measurements presented in this work, other common treatments, such as fine BCP, fine electro polishing and annealing at temperatures above 850 °C, are interesting treatments to investigate. The same applies for more advanced surface alterations such as nitrogen doping and infusion. NTCI can also be used to examine SIS-layered niobium, which is the subject of very recent cavity research. Here, for example, measurements can be done after each layer by introducing

vacuum breaks in-between layers and also the influence of the vacuum-break itself on thermal resistance can be studied.

## ACKNOWLEDGEMENTS

The authors acknowledge the excellent support from DESY (Hamburg, Germany), a member of the Helmholtz Association HGF. This work was supported by the BMBF under the research grants 05K19GUB, 05H2021 and 05K22GUD and by the Helmholtz Association within the topic Accelerator Research and Development (ARD) of the Matter and Technologies (MT) Program. Additionally the authors would like to thank Rezvan Ghanbari (UHH), who helped to prepare the samples, and Isabel Gonzalez Diaz-Palacio and Lea Preece (both UHH) for coating the samples to be measured.

## REFERENCES

- [1] J. Amrit and M. X. François, “Heat Flow at the Niobium-Superfluid Helium Interface: Kapitza Resistance and Superconducting Cavities”, *J. Low Temp. Phys.*, vol. 119, pp. 27–40, 2000. doi:10.1023/A:1004604401306
- [2] J. Amrit and C. Z. Antoine, “Kapitza resistance cooling of single crystal (111) niobium for superconducting rf cavities”, *Phys. Rev. Spec. Top. Accel. Beams*, vol. 13, no. 2, p. 023201, 2010. doi:10.1103/PhysRevSTAB.13.023201
- [3] S. W. Van Sciver, *Helium Cryogenics*, Plenum Press, 1986, pp. 143–144.
- [4] F. Koechlin and B. Bonin, “Parametrization of the niobium thermal conductivity in the superconducting state”, *Supercond. Sci. Technol.*, vol. 9, no. 6, p. 453, 1996. doi:10.1088/0953-2048/9/6/003